



ChemComm

Single molecule magnet behaviour in a square planar $S = 1/2$ Co(II) complex and spin-state assignment of multiple relaxation modes

Journal:	<i>ChemComm</i>
Manuscript ID	CC-COM-03-2020-001854.R1
Article Type:	Communication

SCHOLARONE™
Manuscripts

Single molecule magnet behaviour in a square planar $S = 1/2$ Co(II) complex and spin-state assignment of multiple relaxation modes

Received 00th January 20xx,
Accepted 00th January 20xx

Indrani Bhowmick^a, David W. Shaffer^b, Jenny Y. Yang^b, Matthew P. Shores^{a*}

DOI: 10.1039/x0xx00000x

www.rsc.org/

We report the first example of field-induced single molecule magnet (SMM) behaviour in a square-planar $S = 1/2$ Co(II) pincer complex $[(P^N N^N P)CoBr]Br$ (2**). The related five-coordinate complexes $[(P^C N^C P)CoBr_2]$ (**1**) and $[(P^O N^O P)CoBr_2]$ (**3**) also exhibit SMM properties. Partial spin crossover displayed by **3** allows for assignment of distinct relaxation modes to each spin state.**

Recently, several $3d$ metal-based mononuclear complexes have been reported that possess only one unpaired electron, yet nevertheless exhibit slow relaxation of magnetization under applied static magnetic field. These $S = 1/2$ single molecule magnets (SMMs) feature low-spin V(IV),¹ Mn(IV),² and Fe(III);³ spin-crossover Co(II);⁴ Ni(I);⁵ low-spin Ni(III);⁶ Cu(II)⁷ ions. Theoretically, the well-known Orbach relaxation mechanism observed in most classical SMMs is not possible for an $S = 1/2$ system due to the lack of energy barrier to reverse the spin. Whereas several relaxation processes may be operative, including quantum tunnelling of magnetization (QTM) and/or direct relaxation processes, in most cases, the magnetic dynamics for $S = 1/2$ SMMs are dominated by Raman relaxation.

The SMM properties of high-spin $S = 3/2$ Co(II) complexes are well-studied over the last few years. Besides being the largest class of $3d$ -based mononuclear SMMs, many Co(II) complexes can also exhibit spin-crossover (SCO) between high-spin $S = 3/2$ and low-spin $S = 1/2$ states,^[4, 8] or have a low-spin $S = 1/2$ ground state. The magnetic relaxation properties of the $S = 1/2$ ground state can be particularly interesting for development of electron spin-based qubits, as highlighted in recent molecular quantum computation investigations.⁹

In this communication, we aim to identify correlations between spin states of Co(II) ($S = 3/2$ and/or $S = 1/2$) and magnetic relaxation dynamics. We uncover and explore slow magnetic relaxation behaviour for a series of Co(II) complexes (**1-3**) featuring neutral pincer ligands with molecular formula

$Co(t-Bu)_2P^E Py^E P(t-Bu)_2 Br_2$, where Py = pyridine, E = CH₂, NH, and O, respectively.^{10b} We previously found that a small change of the electronics of the non-bridging atoms was sufficient to change the coordination geometry and spin state of the Co(II) ion (Fig. 1).^{10a} Compounds **1** and **3** are neutral penta-coordinate species, with two bromides coordinated to Co(II), whereas in compound **2** one bromide is bound to Co(II) to form a square-planar monocationic complex, and the other bromide balances charge in the lattice.

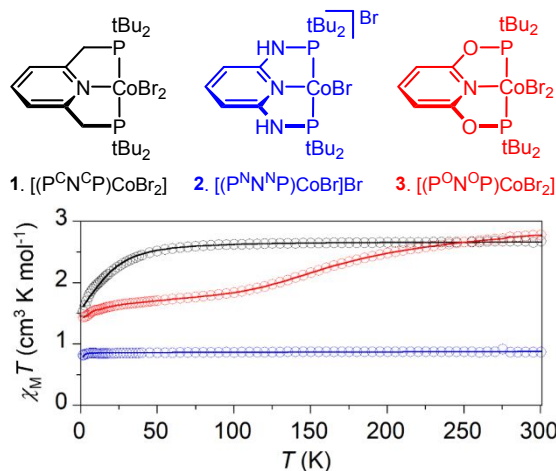


Fig. 1 Top: pentacoordinate compounds **1** and **3** and square planar compound **2**. **Bottom:** The $\chi_M T$ vs. T data show **1** as high spin, **2** as low spin and **3** as partial (~50%) spin-crossover. Data are reproduced from ref 10.

Given the variability of coordination modes, spin states and electronic structures available, we undertook a deeper investigation of the dynamic magnetic properties of these complexes. This report of SMM dynamics of compounds **1-3** doubles the number of Co(II) low spin square pyramidal complexes known to be SMMs.⁴ We also disclose the first (to our knowledge) $S = 1/2$ SMM for a square planar Co(II) complex (**2**). Furthermore, we use the properties of high-spin **1** and low-spin **2** to connect dynamic magnetic properties to spin-state equilibria in the partial-SCO complex **3**.

^a Department of Chemistry, Colorado State University, Fort Collins, CO, 80523-1872, USA, E-mail: matthew.shores@colostate.edu

^b Department of Chemistry, University of California, Irvine, CA, 92697, USA

*For Electronic Supplementary Information (ESI) and other details see DOI: 10.1039/x0xx00000x

All the magnetic measurements were performed on microcrystalline samples of **1**·0.25CH₂Cl₂, **2**-EtOH and **3** (Fig. S1). The ac magnetic data were collected between 0.1 Hz and 1488 Hz with an oscillating field of 4 Oe. Acknowledging that applied dc fields may influence intermolecular magnetic interactions,^{12b, 11a-c, 13} we chose fields maximize temperature and/or frequency range to probe magnetic dynamics for the slowest processes in a particular energy regime.

For the square-planar complex (compound **2**-EtOH) the room temperature magnetic susceptibility temperature product ($\chi_M T$) value of 0.86 cm³Kmol⁻¹ is much higher than the expected theoretical spin-only value of 0.375 cm³ K mol⁻¹ (for $g = 2$), resulting in an isotropic g value as high as 3.02.¹⁰ The high $\chi_M T$ value could originate from the inherently high magnetic anisotropy of Co(II) that is observed in many Co(II) complexes.^{11a,c, 12} Another contributor is the square planar geometry of Co(II): the orbital angular momentum in the ground state is not quenched by the ligand field, and therefore leads to a large anisotropy; in addition, the low coordination numbers minimize the ligand field relative to the spin-orbit coupling and thus enhance the magnetic anisotropy.

Although square planar **2**-EtOH shows no slow magnetic relaxation at zero applied field, field-dependent in-phase (χ') and out-of-phase (χ'') components of ac magnetic susceptibility are observed at 1.8 K (Fig. S2). With increasing applied dc field, the magnitude of χ'' response increases until 2500 Oe, and maxima shift to lower frequencies. Above 2500 Oe the magnitude of χ'' continues to increase, but more gradually; meanwhile, the maxima shift to higher frequencies. Since the magnetic dynamics are slowest at an applied dc field of 2500 Oe, we measured temperature and frequency dependencies of dynamic magnetic susceptibility at 2500 Oe between 1.8 K and 10.0 K (Figs. 2, S3).

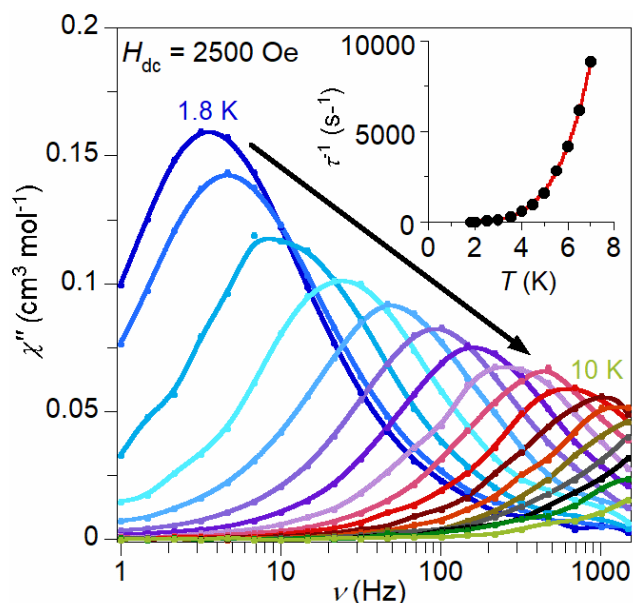


Fig. 2 Temperature and frequency dependencies of out-of-phase (χ'') components of ac magnetic susceptibility for **2**-EtOH, collected between 1.8 and 10 K at dc applied fields of 2500 Oe. **Inset:** Temperature dependence of the relaxation time plotted as τ^{-1} vs T (solid black circles), with the solid red line indicating the fit of the data to the equation $\tau^{-1} = AT^n$, where $n \sim 5$ indicates dominant Raman contributions to the relaxation.

The relaxation time (τ) of **2**-EtOH is deduced as a function of the temperature ($\tau(T) = 1/(2\pi\nu)$) from the maximum of $\chi''(\nu)$ curves at different temperatures (Fig. 2) and the temperature dependence of the relaxation time is modelled by Raman-like relaxation $\tau^{-1} = AT^n$. The fit is in accordance with the entire range of temperature, giving parameters $A = 0.65(2) \text{ s}^{-1}\text{K}^{-4.89}$ and exponent $n = 4.89$ (Table 1). That the value of n is lower than 9 for a Kramers ion ($S = 1/2$) indicates the Raman relaxation process may involve both acoustic (lattice) and optical (molecular) vibrations, as observed in other 3d-based $S = 1/2$ SMM-like systems.^{1,2,6} Attempts to include other relaxation pathways, such as direct or QTM mechanisms, afford unrealistic fitting parameters; thus we conclude that the temperature dependence of relaxation time of **2**-EtOH falls clearly into a Raman-like mechanism. The minimal field dependence of the χ'' (Fig. S2) also supports the assignment of Raman-type spin lattice relaxation in square planar **2**.

Meanwhile, the 5-coordinate Co(II) complexes show multiple relaxation pathways. The $\chi_M T$ vs T plot for **1**·0.25CH₂Cl₂ (Fig. 1) shows that Co(II) retains high spin $S = 3/2$ configuration through the entire range of temperature, and possesses large axial anisotropy ($|D| = 22.324(2) \text{ cm}^{-1}$) and a small rhombic anisotropy ($|E| = 2.404(2) \text{ cm}^{-1}$).^{10a} The field-dependent χ' and χ'' components are collected between 0 Oe and 10000 Oe at 1.8 K (Fig. 3(top) and S4). At zero applied dc field there is no evidence of slow relaxation of magnetization. Upon application of a small dc field, we observe two relaxation events: one between 0.1-1 Hz (low-frequency relaxation, **1**·lfr) and the other one between 100-1488 Hz (high-frequency relaxation, **1**·hfr). At 1000 Oe applied field the **1**·hfr is the dominant relaxation mode, while the **1**·lfr becomes evident at and above 2000 Oe. Interestingly, a larger dc field for $\chi''(\text{1·lfr})$ and $\chi''(\text{1·hfr})$ results in increased intensities until 4000 Oe. The χ'' maxima display anomalous field-dependent trends: the $\chi''_{\text{max}}(\text{1·lfr})$ moves to lower frequencies, indicating slower relaxation; but the $\chi''_{\text{max}}(\text{1·hfr})$ moves to higher frequencies, indicating faster relaxation. Similar field-dependent multiple relaxation modes have been observed several five-coordinate cobalt(II) SMM complexes¹¹ and other mononuclear SMM systems featuring Ni(II), Mn(II) and Cu(II) ions.¹³

Above 4000 Oe, $\chi''_{\text{max}}(\text{1·hfr})$ continues to shift to higher frequencies but with decreasing intensity. The **1**·hfr mode shows the highest magnitude of $\chi''_{\text{max}}(\text{1·hfr})$ at 4000 Oe, therefore, further temperature and frequency-dependent χ' and χ'' data are collected at 4000 Oe between 1.8 to 7.0 K (Fig. S5). At 4000 Oe the $\chi''(\nu)$ shows the presence of **1**·lfr mode along with **1**·hfr below 4.5 K where at higher temperatures only the **1**·hfr pathway is observed. To probe the relaxation dynamics of **1**·hfr mode, the temperature dependent relaxation time (τ) of **1** is deduced as $\tau_{\text{1·hfr}}(T) = 1/(2\pi\nu)$ from the maximum of $\chi''(\nu)$ curves at 4000 Oe (Fig. S6). The relaxation data fit best to a combination of Orbach and QTM pathways, with the equation $\tau_{\text{1·hfr}}^{-1}(T) = \tau_{\text{QTM}}^{-1} + \tau_0^{-1}\exp(-U_{\text{eff}}/k_B T)$, where the τ_{QTM} is relaxation time of QTM, τ_0 is the pre-exponential constant and U_{eff} is the energy needed to reverse the magnetization according to Orbach relaxation

process (Fig. S6). The fit provides $\tau_{\text{QTM}} = 4.36 \times 10^{-4}$ s, $\tau_0 = 4.72 \times 10^{-6}$ s and $U_{\text{eff}} = 9.17$ cm⁻¹ (Table 1).

From the static magnetic properties of the partial spin-crossover compound **3**, we previously estimated that 50% of the Co(II) ions show temperature-dependent SCO ($S = 3/2$ to $S = 1/2$) whereas the remainder retains the high-spin state.¹⁰ The field-dependent χ' and χ'' components of ac magnetic susceptibility are collected at different dc fields between 0 Oe and 6000 Oe at 1.8 K (Fig. 3 (bottom) and S7).

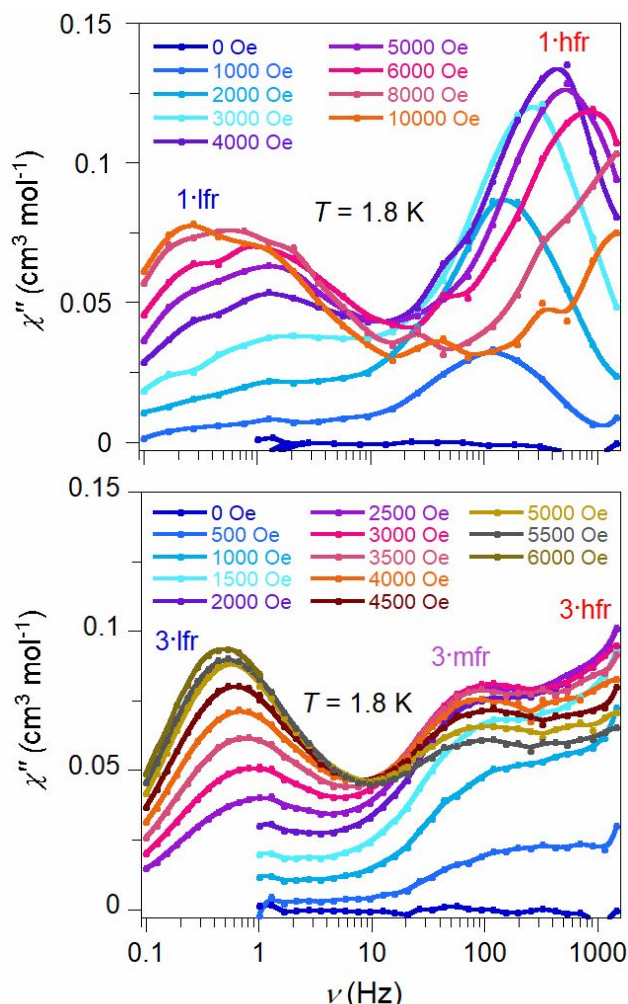


Fig. 3 Frequency dependencies of out-of-phase (χ'') components of ac (oscillating field 4 Oe) magnetic susceptibility of **1·0.25CH₂Cl₂** (top) and **3** (bottom), collected at multiple static dc fields at 1.8 K, showing the presence of multiple non-independent relaxation pathways, where lfr = low-frequency relaxation, mfr = medium-frequency relaxation and hfr = high-frequency relaxation

At zero applied dc field, there is no residual magnetization, but the slow dynamics of magnetization are observed at applied dc fields at and above 500 Oe for **3**. These fields and frequency-dependent χ'' components show three relaxation pathways at 1.8 K (Fig. 3 (bottom), and S7): first between 0.1-1 Hz (**3·lfr**), second between 30-300 Hz (medium frequency relaxation, **3·mfr**) and a third process above 300 Hz (**3·hfr**), measuring the maxima of which is outside the range of our data collection window. At applied fields smaller than 1000 Oe, the **3·mfr** and the **3·hfr** channels are the dominant magnetic dynamic modes, while the **3·lfr** mode becomes significant in applied fields larger than 1000 Oe. At the applied

field of 2500 Oe, the presence of these three relaxation modes is clear, whereas with further increases of applied field the intensity of the **3·lfr** mode significantly increases and **3·mfr** mode decreases and/or overlaps with the **3·hfr** pathway (Fig. S8).

For **3**, the temperature and frequency-dependent χ' and χ'' data are collected at 2500 Oe (Fig S9) as the **3·hfr** data show largest χ'' signals here (Fig S8). Above 2.7 K the **3·lfr** and **3·mfr** pathways are insignificant and only **3·hfr** mode is dominating. Meanwhile, the χ' and χ'' data collected at 5500 Oe – **3·lfr** shows the slowest and maximum responses at that field – between 1.8 and 3.8 K (Fig. S10) show **3·lfr** pathway as dominant until 3.8 K, but the **3·mfr** pathway diminishes after 3 K. Thus, the **3·hfr** mode becomes the dominant pathway at higher temperatures. The $\tau_{3\cdot\text{lfr}}(T) = 1/(2\pi\nu)$ are deduced from the maximum of $\chi''(\nu)$ curves at 5500 Oe (Fig. S11), and the data best fit to an Orbach-only relaxation as $\tau_{3\cdot\text{lfr}}(T)^{-1} = \tau_0^{-1} \exp(-U_{\text{eff}}/k_B T)$, giving $\tau_0 = 5.51 \times 10^{-3}$ s and $U_{\text{eff}} = 4.87$ cm⁻¹ (Table 1). We note that the U_{eff} value is very small, which has been observed in case of large positive anisotropy (D); but attempts to fit the $\tau_{3\cdot\text{lfr}}(T)$ data to other models resulted in inferior or nonsensical fitting parameters (Fig S12).

The field-dependent relaxation times for compound **1·0.25CH₂Cl₂** are deduced as $\tau(H) = 1/(2\pi\nu)$ from the maximum of $\chi''_{\text{max}}(\mathbf{1}\cdot\text{lfr}$ or $\mathbf{1}\cdot\text{hfr})$ at different applied dc fields and plotted in Fig. 4 (left). Qualitatively, the **1·hfr** and **1·lfr** events are increasing and decreasing, respectively, as the applied field increases. Similarly, for compound **3**, the $(\tau(H) \text{ vs } H)$ data at 1.8 K show that the **3·lfr** pathway becomes slower with the increase of the applied field, whereas the **3·mfr** mode is only weakly influenced by increasing field (Fig. 4 (right)). The presence of low, intermediate and high frequency relaxation modes exhibiting field dependence has been observed in some mononuclear SMM systems.^{11, 13} Similar to our system (**1** and **3**), some Co(II)¹¹ and Ni(II)^{13b,c} SMMs show prolongation and acceleration of relaxation times for the low and high frequency modes, respectively, as the applied dc field is increased.

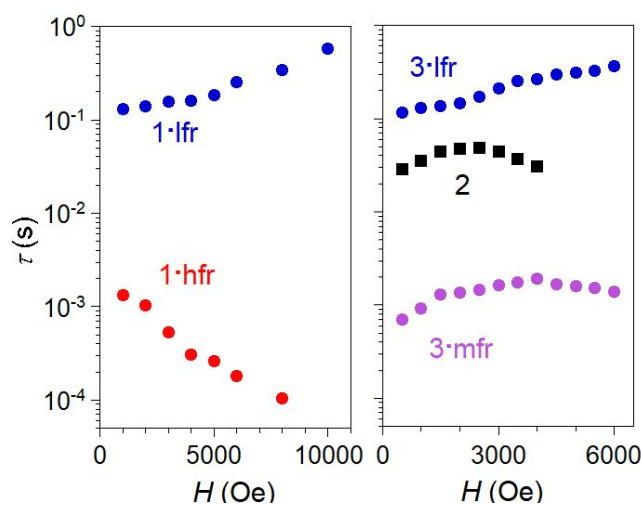


Fig. 4 Field dependencies of relaxation events for **1-3**, collected at 1.8 K. Left: For **1·0.25CH₂Cl₂**, the high-frequency-relaxation (**1·hfr**, solid red circles) and low-frequency-relaxation (**1·lfr**, solid blue circles) phenomena diverge as the field is increased. Right: For compound **3**, the medium-frequency relaxation (**3·mfr**, solid purple circles)

phenomenon changes less significantly whereas the low-frequency-relaxation (3'fhr, solid blue circles) phenomenon becomes slower; 3'hfr for this complex is not observed at 1.8 K although the 3'hfr phenomenon (Fig. 3 bottom) appears to be faster with increase of applied field. For comparison, black squares represent the single relaxation event observed for 2-EtOH.

Interestingly, we observe one relaxation mode for compound 2-EtOH (LS, $S = 1/2$), two relaxation modes for compound 1-0.25CH₂Cl₂ (HS, $S = 3/2$) and three relaxation modes for compound 3 (1:1 LS:HS); see Table 1. At a fixed temperature, 1.8 K, the field dependence of the relaxation time ($\tau(H)$ vs H) of 2-EtOH (black square in Fig. 4(right)) is minimal and qualitatively similar to the 3'mfr mode of 3 showing predominantly a Raman-like relaxation. This data suggest an interesting connection between the spin states and the magnetic dynamics of these three complexes, where we attribute the 3'mfr relaxation mode of the compound 3 to the SCO-active Co(II) ion, and the 3'fhr+3'hfr mode the high spin Co(II) counterpart.

Table 1. The spin state and relaxation mode correlation

Compound	1-0.25CH ₂ Cl ₂	2-EtOH	3
Low-temperature spin state	high spin (HS)	low spin (LS)	1:1 HS: LS
Number of relaxation modes	2	1	3
Regions of relaxation modes (Hz)	>100 (1'hfr) 0.1-1 (1'fhr)	1-10 (mfr)	>300 (3'hfr) 30-300 (3'mfr) 0.1-1 (3'fhr)
Orbach relaxation	(1'hfr) $\tau_0 = 4.72 \times 10^{-6}$ s $U_{\text{eff}} = 9.17$ cm ⁻¹	N/A	(3'fhr) $\tau_0 = 5.51 \times 10^{-3}$ s $U_{\text{eff}} = 4.87$ cm ⁻¹
QTM (τ_{QTM})	4.36×10^{-4} s	N/A	N/A
Raman relaxation	N/A	$A = 0.65$ s ⁻¹ K ^{-4.89} $n = 4.89$	N/A

In this communication, we have disclosed the magnetic dynamics of three Co(II) complexes where the relaxation pattern of compound 3 (HS+SCO) can be qualitatively assigned as a combination of high- and low-spin species, as exemplified in compounds 1 (HS) and 2 (LS). Differences in the coordinating ligand sets and coordination geometries undoubtedly influence the magnitudes of relaxation times observed, which may manifest as comparable but non-superimposable $\tau(H)$ values. Notwithstanding, we surmise that the dynamic modes of the high- and low-spin species are largely independent of each other. This communication indicates the need for further systematic studies on high- and low-spin cobalt complexes to verify our hypothesis on the spin state correlation with magnetic relaxation dynamics; it may lead us closer to predicting dynamic magnetic properties just by knowing the spin state of the molecule.

Acknowledgments

We thank Colorado State University and the National Science Foundation (CHE-1363274 and CHE-1800554 for MPS and IB; CAREER CHE-1554744 for DWS and JYY) for financial support.

Conflicts of interest

There are no conflicts to declare.

Notes and references

- (a) L. Tesi, E. Lucaccini, I. Cimatti, M. Perfetti, M. Mannini, M. Atzori, E. Morra, M. Chiesa, A. Caneschi, L. Sorace, R. Sessoli, *Chem. Sci.*, 2016, **7**, 2074–2083; (b) M. Atzori, L. Tesi, E. Morra, M. Chiesa, L. Sorace, R. Sessoli, *J. Am. Chem. Soc.*, 2016, **138**, 2154–2157. (c) M. Atzori, L. Tesi, S. Benci, A. Lunghi, R. Righini, A. Taschin, R. Torre, L. Sorace, R. Sessoli, *J. Am. Chem. Soc.*, 2017, **139**, 4338–4341; (d) M. Atzori, E. Morra, L. Tesi, A. Albino, M. Chiesa, L. Sorace, R. Sessoli, *J. Am. Chem. Soc.*, 2016, **138**, 11234–11244; (e) M. Atzori, S. Benci, E. Morra, L. Tesi, M. Chiesa, R. Torre, L. Sorace, R. Sessoli, *Inorg. Chem.*, 2018, **57**, 731–740; (f) D. Stingen, M. Atzori, C. M. Fernandes, R. R. Ribeiro, E. L. de Sá, D. F. Back, S. O. K. Giese, D. L. Hughes, G. G. Nunes, E. Morra, M. Chiesa, R. Sessoli, J. F. Soares, *Inorg. Chem.*, 2018, **57**, 1393–11403.
- M. Ding, G. E. Cutsail III, D. Aravena, M. Amoza, M. Rouzières, P. Dechambenoit, Y. Losovyj, M. Pink, E. Ruiz, R. Clérac, J. M. Smith, *Chem. Sci.*, 2016, **7**, 6132–6140.
- A. B. Buades, V. S. Arderiu, L. Maxwell, M. Amoza, D. Choquesillo-Lazarte, N. Aliaga-Alcalde, C. Viñas, F. Teixidor, E. Ruiz, *Chem. Commun.*, 2019, **55**, 3825–3828.
- (a) H.-H. Cui, J. Wang, X.-T. Chen, Z.-L. Xue, *Chem. Commun.*, 2017, 53, 9304–9307; (b) L. Chen, J. Song, W. Zhao, G. Yi, Z. Zhou, A. Yuan, Y. Song, Z. Wang, Z.-W. Ouyang, *Dalton Trans.*, 2018, 47, 16596–16602.
- (a) R. C. Poulten, M. J. Page, A. G. Algarra, J. J. Le Roy, I. López, E. Carter, A. Llobet, S. A. Macgregor, M. F. Mahon, D. M. Murphy, M. Murugesu, M. K. Whittlesey, *J. Am. Chem. Soc.*, 2013, **135**, 13640–13643; (b) W. Lin, T. Bodenstern, V. Mereacre, K. Fink, A. Eichhöfer, *Inorg. Chem.*, 2016, **55**, 2091–2100.
- I. Bhowmick, A. J. Roehl, J. R. Neilson, A. K. Rappé, M. P. Shores, *Chem. Sci.*, 2018, **9**, 6564–6571.
- R. Boča, C. Rajnák, J. Titiš, D. Valigura, *Inorg. Chem.*, 2017, **56**, 1478–1482.
- (a) H. A. Goodwin, *Top. Curr. Chem.*, 2004, **234**, 23; (b) I. Krivokapic, M. Zerara, M. L. Dakua, A. Vargas, C. Enachescu, C. Ambrusc, P. Tregenna-Piggott, N. Amstutz, E. Krausz and A. Hauser, *Coord. Chem. Rev.*, 2007, **251**, 364–378; (c) S. Hayami, Y. Komatsu, T. Shimizu, H. Kamihata and Y. H. Lee, *Coord. Chem. Rev.*, 2011, **255**, 1981–1990; (d) R. G. Miller, S. Narayanaswamy, J. L. Tallon and S. Brooker, *New J. Chem.*, 2014, **38**, 1932; (e) B. Brachňáková, I. Šalitroš, *Chem. Pap.*, 2018, **72**, 4, 773–798. (f) O. Drath, C. Boskovic, *Coord. Chem. Rev.*, 2018, **375**, 256–266.
- (a) Y.-S. Ding, Y.-F. Deng and Y.-Z. Zheng, *Magnetochemistry*, 2016, **2**, 40 (1-19). (b) E. Moreno-Pineda, C. Godfrin, F. Balestro, W. Wernsdorfer, M. Ruben, *Chem. Soc. Rev.*, 2018, **47**, 501–513. (c) L. Tesi, E. Lucaccini, I. Cimatti, M. Perfetti, M. Mannini, M. Atzori, E. Morra, M. Chiesa, A. Caneschi, L. Sorace and R. Sessoli, *Chem. Sci.*, 2016, **7**, 2074–2083. (d) R. Sessoli, *ACS Cent. Sci.*, 2015, **1**, 473–474.
- (a) D. W. Shaffer, I. Bhowmick, A. L. Rheingold, C. Tsay, B. N. Livesay, M. P. Shores, J. Y. Yang, *Dalton Trans.*, 2016, **45**, 17910–17917. (b) D. W. Shaffer, S. I. Johnson, A. L. Rheingold, J. W. Ziller, W. A. Goddard, R. J. Nielsen, and J. Y. Yang, *Inorg. Chem.*, 2014, **53**, 13031–1304.
- (a) A. Świtlicka, B. Machura, M. Penkala, A. Bieńko, D. C. Bieńko, J. Titiš, C. Rajnák, R. Boča, A. Ozarowski, M. Ozero, *Inorg. Chem.*, 2018, **57**, 12740–12755; (b) C. Rajnák, J. Titiš, J. Miklovič, G. E. Kostakis, O. Fuhr, M. Ruben, R. Boča, *Polyhedron*, 2017, **126**, 174–183; (c) C. Rajnák, J. Titiš, O. Fuhr, M. Ruben, R. Boča, *Inorg. Chem.*, 2014, **53**, 8200–8202. (d) O. Y. Vassilyeva, E. A. Buvaylo, V. N. Kokozay, B. W. Skelton, C. Rajnák, J. O. Titiš, R. Boča, *Dalton Trans.*, 2019, **48**, 11278–11284.
- (a) F. Habib, O. R. Luca, V. Vieru, M. Shiddiq, I. Korobkov, S. I. Gorelsky, M. K. Takase, L. F. Chibotaru, S. Hill, R. H. Crabtree, M. Murugesu, *Angew. Chem. Int. Ed.*, 2013, **52**, 11290–11293. (b) F. Habib, I. Korobkova, M. Murugesu, *Dalton Trans.*, 2015, **44**, 6368–6373.
- (a) Y. P. Tupolova, I. N. Shcherbakov, L. D. Popov, V. E. Lebedev, V. V. Tkachev, K. V. Zakharov, A. N. Vasiliev, D. V. Korchagin, A. V. Palii, S. M. Aldoshin, *Dalton Trans.*, 2019, **48**, 6960–6970; (b) J. Titiš, C. Rajnák, D. Valigura, R. Boča, *Dalton Trans.*, 2018, **47**, 7879–7882; (c) J. Titiš, V. Chrenková, C. Rajnák, J. Moncol, D. Valigura, R. Boča,

Journal Name

COMMUNICATION

Dalton Trans., 2019, **48**, 11647–11650; (d) R. Boca, C. Rajnak, J. Titiš, D. Valigura, *Inorg. Chem.*, 2017, **56**, 1478–1482. (e) C. Rajnák, J. Titiš, J. Moncol, R. Mičová, R. Boča, *Inorg. Chem.*, 2019, **58**, 991–994.

TOC: First reports of square planar $S = 1/2$ Co(II) single molecule magnet, and spin state assignment to the multiple relaxation modes of a structurally related spin crossover Co(II) complex.

